Supporting Information
Rational design of red-shifted 1,2-azaborinine-based molecular solar thermals

Adrian J. Müller, Johannes Markhart, Holger F. Bettinger, and Andreas Dreuw

Contents

1 Molecule generation and ground state energies

Force-field optimised molecules were generated from SMILES strings using the RDKit [1] library.
Subsequently, they were optimised at the PBEh-3c/def2-mSVP [2] level of theory. Frequency analyses were performed to confirm local minima with no imaginary frequencies. Single point energies were obtained at the revPBE0 [3,4](D3BJ) [5]/def2-TZVP [6] level of theory. These steps were conducted in the Orca 6.0.1 [7,8] program package. This combination of density functional theory (DFT) functionals was chosen based on an initial benchmark of 1,2-dihydro-1,2-azaborine **1** against coupled cluster singles-doubles-perturbative-triples CCSD(T) [9] reference values where revPBE0(D3BJ)/def2-TZVP//PBEh-3c/def2-mSVP corrected by the zero point vibrational energies (ZPVE) at the PBEh-3c/def2-mSVP level performed best. The results of the benchmark are summarised in Table 1.

Table 1: Comparison of revPBE0(D3BJ)/def2-TZVP//PBEh-3c/def2-mSVP (DFT) with CCSD(T) reference values [10]

Structure	$E_{\mathrm{rel,DFT}}/\mathrm{kcal\,mol^{-1}}$	$E_{\mathrm{rel,CCSD(T)}}/\mathrm{kcal\,mol^{-1}}$
BNB	-59.6	-59.3
TS1	21.4	22.2
PF	17.1	17.8
TS2	18.6	19.1
BND	0.0	0.0

2 Excited states

A full linear response time-dependent DFT (LR-TDDFT) approach was chosen to compute the first three vertical singlet excitation energies which were computed at the BNB ground state equilibrium geometries of the compounds. Energies were benchmarked against *ab initio* vertical excitation energies obtained from the algebraic diagrammatic construction scheme up to third-order ADC(3)[11] with the def2-TZVP basis set (see Table 2). The combination of ωB97X-D[12]/def2-TZVP performed best and was chosen for all further excited state computations. This benchmark was extended for compound **2** (4-CN-5-OH), which is summarised in Table 3. These computations were performed in the Q-Chem 6.2 software package[13].

Table 2: Vertical excitation energies of **1-BNB** with their corresponding oscillator strengths in parentheses

State	ADC(3)/eV	Full ωB97X-D/eV
S_1	4.91 (0.16)	5.17 (0.17)
S_2	5.95 (0.05)	6.18 (0.09)
S_3	6.39 (0.00)	6.62 (0.00)

Table 3: Vertical excitation energies of **2-BNB** with their corresponding oscillator strengths in parentheses

State	ADC(3)/eV	Full ωB97X-D/eV
S_1	4.01 (0.14)	4.07 (0.13)
S_2	5.62 (0.02)	5.76 (0.00)
S_3	6.11 (0.00)	6.27 (0.00)

3 Collected data

3.1 Substitution site screening

Either a methoxy or cyano group was substituted at each possible position of the BNB parent molecule **1**. The vertical excitation energies of the first singlet excited state at the full TDDFT level of theory at their ground state equilibrium geometries are summarised in Table 4.

Table 4: Substitution site screening of the first vertical excitation energies at BNB equilibrium structures with a cyano or methoxy group

Position	CN/eV	OMe/eV
1	4.89	5.07
2	4.99	4.92
3	4.82	4.89
4	4.79	5.29
5	5.14	4.73
6	4.88	4.97

3.2 Compound screening

Table 5: Collected TDDFT vertical excitation energies of the first singlet excited state S_1 and oscillator strengths f_{osc} of the screened molecules with their spectral separation ΔS_1, their storage energies E_{S}, and push-pull classifier

	BNB		BND				
molecule	S_1/eV	f_{osc}	S_1/eV	f_{osc}	ΔS_1/eV	E_{S}/kcal mol^{-1}	class
4CF3-5H	5.06	0.16	5.79	0.03	0.73	58.4	noM
4CF3-5Me	4.86	0.15	5.75	0.05	0.89	52.8	noM
4CF3-5NH2	4.88	0.16	5.33	0.06	0.45	45.7	push
4CF3-5NMe2	4.63	0.00	4.96	0.10	0.33	44.3	push
4CF3-5OH	4.56	0.14	5.62	0.03	1.07	48.4	push
4CF3-5OMe	4.75	0.15	5.44	0.06	0.69	49.1	push
4CHO-5H	3.76	0.00	3.54	0.00	-0.23	60.9	pull
4CHO-5Me	3.57	0.00	3.59	0.00	0.02	52.0	pull
4CHO-5NH2	3.30	0.09	3.95	0.00	0.64	46.0	p-p
4CHO-5NMe2	3.40	0.01	3.99	0.00	0.59	40.9	p-p
4CHO-5OH	3.48	0.09	3.71	0.00	0.23	57.7	p-p
4CHO-5OMe	3.92	0.09	3.84	0.00	-0.08	47.9	p-p
4Cl-5H	5.20	0.15	5.69	0.03	0.49	58.1	noM
4Cl-5Me	5.02	0.15	5.58	0.04	0.55	54.3	noM

Continued on next page

Table 5 – continued from previous page

	BNB		BND				
molecule	S_1/eV	f_{osc}	S_1/eV	f_{osc}	ΔS_1/eV	$E_{\mathrm{S}}/\mathrm{kcal\,mol^{-1}}$	class
4Cl-5NH2	5.05	0.15	5.11	0.03	0.06	49.9	push
4Cl-5NMe2	4.52	0.07	4.85	0.06	0.33	48.0	push
4Cl-5OH	4.58	0.15	5.33	0.02	0.75	53.7	push
4Cl-5OMe	4.95	0.14	5.20	0.04	0.25	52.3	push
4CN-5H	4.79	0.15	5.38	0.07	0.59	57.7	pull
4CN-5Me	4.58	0.14	5.34	0.12	0.75	53.5	pull
4CN-5NH2	3.81	0.11	4.96	0.13	1.15	47.0	p-p
4CN-5NMe2	3.96	0.07	4.68	0.18	0.71	42.2	p-p
4CN-5OH	4.07	0.13	5.21	0.10	1.15	52.2	p-p
4CN-5OMe	4.24	0.13	5.07	0.15	0.83	49.6	p-p
4COOH-5H	4.58	0.12	4.96	0.01	0.38	58.5	pull
4COOH-5Me	4.47	0.13	5.05	0.03	0.59	51.1	pull
4COOH-5NH2	3.55	0.10	4.80	0.15	1.25	43.9	p-p
4COOH-5NMe2	4.67	0.07	4.61	0.26	-0.06	41.2	p-p
4COOH-5OH	3.66	0.11	5.13	0.11	1.47	55.5	p-p
4COOH-5OMe	4.41	0.12	4.96	0.13	0.55	43.7	p-p
4DCV-5H	3.97	0.05	4.02	0.31	0.05	54.4	pull
4DCV-5Me	3.89	0.04	4.08	0.50	0.20	47.7	pull
4DCV-5NH2	3.53	0.06	3.48	0.37	-0.04	37.1	p-p
4DCV-5NMe2	3.49	0.06	3.20	0.31	-0.28	40.5	p-p
4DCV-5OH	3.77	0.04	3.98	0.54	0.21	42.7	p-p
4DCV-5OMe	3.84	0.04	3.87	0.60	0.03	42.4	p-p
4F-5H	5.41	0.15	5.85	0.01	0.44	59.8	noM
4F-5Me	5.25	0.15	5.69	0.02	0.44	57.1	noM
4F-5NH2	4.65	0.11	5.22	0.02	0.58	55.0	push
4F-5NMe2	4.71	0.07	4.89	0.03	0.18	52.6	push
4F-5OH	4.85	0.14	5.45	0.01	0.60	58.3	push
4F-5OMe	5.17	0.14	5.34	0.02	0.17	53.4	push
4H-5H	5.17	0.17	5.68	0.02	0.52	59.6	noM
4NO2-5H	4.03	0.00	4.00	0.00	-0.03	59.5	pull
4NO2-5Me	4.16	0.02	4.06	0.00	-0.09	51.8	pull
4NO2-5NH2	3.55	0.06	4.26	0.00	0.71	41.8	p-p
4NO2-5NMe2	4.37	0.00	4.11	0.08	-0.25	39.6	p-p
4NO2-5OH	3.30	0.07	4.12	0.00	0.82	54.7	p-p
4NO2-5OMe	4.28	0.01	4.12	0.00	-0.16	47.8	p-p

4 Thermal back reaction of compound 2

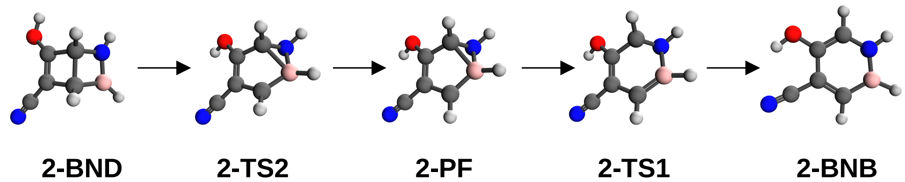

Figure S1: Key optimised structures of the thermal back reaction of compound **2**.

4.1 2-BND

N	-1.62987430677407	0.65910454822546	0.11239829235636
B	-1.60481121891966	-0.66979992319667	0.55200737154452
C	-0.35241833693474	-0.99123406001591	-0.40656304237654
C	1.00750344447715	-0.59452581910339	0.14114126957436
C	1.98975200792001	-1.31931408681468	0.84374066675243
N	2.78498043908664	-1.93591196011677	1.40726964597970
C	0.86801576976356	0.69841920966021	-0.18918180339924
O	1.61735803083730	1.76587038009862	0.04447622237069
C	-0.50252622982680	0.50970873950526	-0.79724017159346
H	-2.08982498418967	1.51922533171208	0.35747757231539
H	-2.29000496119860	-1.24039027647852	1.33662862170411
H	-0.37814022792172	-1.75437509017781	-1.18216159456232
H	1.24659613457182	2.54001648795287	-0.38670735394745
H	-0.66660556089128	0.81320651874919	-1.83328569671854

4.2 2-TS2

N	-1.52375116416901	0.96199955875892	0.53488836482675
B	-1.59424590397458	-0.54668705728682	0.34377441036662
C	-0.30809666669035	-1.25740054520639	0.08072782317166
C	0.97291819257836	-0.54596543188056	0.10636600894318
C	2.22182749318681	-1.04399606137756	0.54457333715010
N	3.25207046959435	-1.41967021769271	0.90160222747876
C	0.68666347495704	0.70859724662084	-0.27763854307123
O	1.36287078225483	1.84246177249793	-0.28696173004782
C	-0.76648366777127	0.69909059035928	-0.59253205764317
H	-2.42536858349889	1.37822823626349	0.34410142813587
H	-2.64389364148334	-1.05002346517618	0.08225723578174
H	-0.32315563040494	-2.26608218395357	-0.32610175410077
H	2.21206604934175	1.74176962976436	0.16045507407828
H	-1.12342120392076	0.79767792830894	-1.61551182506997

4.3 2-PF

N	-1.52127399058083	0.97220550692800	0.51013188125661
B	-1.55985136632061	-0.55573601095980	0.12047544438505
C	-0.29383126235361	-1.35370888494705	0.17286386000321
C	0.92161034494010	-0.59591310080403	0.10624675054127
C	2.21215554046572	-1.01520467067036	0.51754894189070
N	3.27944802124636	-1.30987606145420	0.83958249359077
C	0.63204920352882	0.67497402268884	-0.29482564277746
O	1.36984650582648	1.76177121296154	-0.26341484299478
C	-0.81203906037579	0.78215981798775	-0.64340158971277
H	-2.43326890226600	1.39166501006066	0.37277391970697
H	-2.62072223936856	-1.00506200364082	-0.18406196830351
H	-0.23960666047117	-2.43551061529050	0.09002657601339
H	2.19017690535049	1.61855069622643	0.22779915722998
H	-1.15095103962139	0.97967808091353	-1.65671398082943

4.4 2-TS1

N	-1.61033523706126	0.89943741803331	0.35175982149896
B	-1.58624474947928	-0.73008002420520	0.27439318919992
C	-0.31808549156315	-1.41001264286070	0.16325879847547
C	0.88547315913798	-0.58806446285109	0.09259144401465
C	2.18159377933798	-0.99856668886453	0.50819570185882
N	3.24839208640534	-1.29332075408853	0.83216900754164
C	0.67243726744322	0.67840211871203	-0.28860260028744
O	1.45972818066738	1.76122929273672	-0.28876015793769
C	-0.75375495913527	0.99257399397048	-0.61823062411113
H	-2.52747735059748	1.27497824638814	0.14365228595005
H	-2.70525782877148	-1.11354063348784	0.14518520299132
H	-0.22005684762034	-2.48326752431914	0.07876348887122
H	2.27574940336909	1.58634990698731	0.19603145088031
H	-1.00216141213273	1.42388175384904	-1.59040700894609

4.5 2-BNB

N	-2.27721507429733	-0.00416422546093	-0.00001647257465
B	-1.86771243391399	-1.36394411226129	0.00002810450236
C	-0.36761914276215	-1.55462556803482	0.00007918859972
C	0.43870314473036	-0.44478083615291	0.00007842559277
C	1.86586215596614	-0.56687842956626	0.00010223237943
N	3.01717732714509	-0.61183471857441	-0.00013510129629
C	-0.08373445499075	0.88339808863423	0.00003434942561
O	0.70414738851223	1.97891363163415	0.00004266185024
C	-1.43430933202965	1.05984154795364	-0.00001665522726
H	-3.25755517224377	0.22841844602199	-0.00005246145995
H	-2.69271046110039	-2.22056981315484	0.00001807977160
H	0.11133176768756	-2.52522768986720	0.00012173519089
H	1.63721125089875	1.74302464822244	-0.00002980963990
H	-1.86008920880210	2.05373527230622	-0.00005492261457

5 Conical intersection

A spin-flip TDDFT minimum energy crossing point optimisation was performed using SF-BHHLYP[14](D3BJ)/cc-pVDZ[15]. Additionally, **2** was optimised at BHHLYP(D3BJ)/cc-pVDZ for comparison. Subsequently, vertical exciation energies were obtained at the ωB97X-D/def2-TZVP level of theory. These computations were performed in the Q-Chem 6.2 software package[13].

5.1 S_1/S_0 minimum energy crossing point of compound 2

C	0.0000000000	0.0000000000	0.0000000000
C	0.0000000000	0.0000000000	1.3422460000
O	1.0983672108	0.0000000000	-0.7740087848
H	0.8866486568	0.2440563537	-1.6740348123
C	1.2133667211	0.0052713669	2.0920016498
N	2.1781653173	-0.0001900509	2.7177935015
C	-1.3248651534	0.0424550452	1.9509492958
H	-1.4299625714	-0.3133273454	2.9676070710
B	-2.4463949355	0.4828061738	1.1336385177
H	-3.6205480908	0.3666210854	1.3078880581
C	-1.3416421613	0.0362925454	-0.6397035975
H	-1.5650525416	-0.6645468171	-1.4478332663
N	-2.1389333190	1.0387677257	-0.3366921438
H	-2.9735133333	1.0707184476	-0.9060230002

6 Solvation effects

Azaborinines are commonly dissolved in cyclohexane by the Bettinger group. Hence, the conductor-like polarisable continuum model with parameters corresponding to cyclohexane was employed to estimate solvation effects for compounds **1** and **2**. With the above described workflow, storage energies, spectral separation, and UV/Vis spectra were simulated. A comparison of the results with and without solvent effects is shown in Table 6. The UV/Vis spectra with and without solvation effects are visualised in Fig. S2 and S3. Solvation effects induce minor changes resulting in a slight red-shift, increased oscillator strength, larger spectral separation, and slightly affected storage energies. This justifies our screening in the gas phase and our neglect of solvation effects.

Table 6: Comparison of storage energies, first vertical excitation energies of the first singlet excited state in the BNB form $S_{1,\mathrm{BNB}}$ and corresponding oscillator strengths f_{osc} in parentheses, and the spectral separation ΔS_1 of compounds **1** and **2** in the gas phase and in cyclohexane (cy)

Property	**1** (gas phase)	**1** (cy)	**2** (gas phase)	**2** (cy)
S_1(BNB)/eV	5.17	5.08	4.07	3.97
$f_{\mathrm{osc,S_1(BNB)}}$	0.17	0.20	0.13	0.16
Spectral separation ΔS_1/eV	0.52	0.58	1.15	1.19
E_{S}/kcal mol^{-1}	59.6	60.4	52.2	50.6

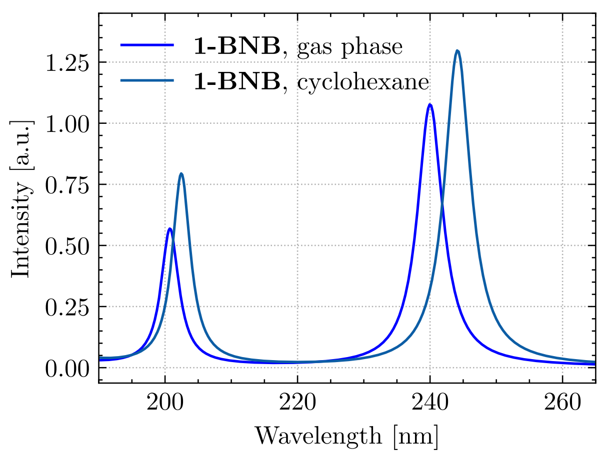

Figure S2: Simulated TDDFT UV/Vis spectra of **1-BNB** in the gas phase and in cyclohexane (full width at half maximum=0.1 eV).

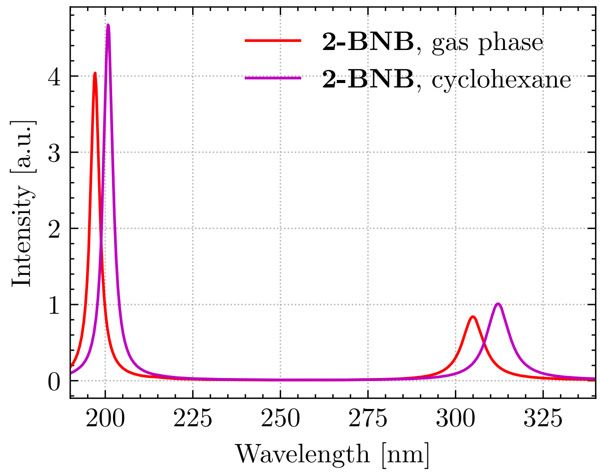

Figure S3: Simulated TDDFT UV/Vis spectra of **2-BNB** in the gas phase and in cyclohexane (full width at half maximum=0.1 eV).

References

[1] G. Landrum, P. Tosco, B. Kelley, R. Rodriguez, D. Cosgrove, R. Vianello, sriniker, P. Gedeck, G. Jones, NadineSchneider, E. Kawashima, D. Nealschneider, A. Dalke, M. Swain, B. Cole, S. Turk, A. Savelev, tadhurst cdd, A. Vaucher, M. Wójcikowski, I. Take, V. F. Scalfani, R. Walker, K. Ujihara, D. Probst, J. Lehtivarjo, H. Faara, g. godin, A. Pahl and J. Monat, *RDKit: Open-source cheminformatics*, 2025, `https://zenodo.org/records/14779836`.

[2] S. Grimme, J. G. Brandenburg, C. Bannwarth and A. Hansen, *J. Chem. Phys.*, 2015, **143**, 054107.

[3] Y. Zhang and W. Yang, *Phys. Rev. Lett.*, 1998, **80**, 890–890.

[4] C. Adamo and V. Barone, *J. Chem. Phys.*, 1999, **110**, 6158–6170.

[5] S. Grimme, S. Ehrlich and L. Goerigk, *J. Comput. Chem.*, 2011, **32**, 1456–1465.

[6] F. Weigend and R. Ahlrichs, *Phys. Chem. Chem. Phys.*, 2005, **7**, 3297–3305.

[7] F. Neese, F. Wennmohs, U. Becker and C. Riplinger, *J. Chem. Phys.*, 2020, **152**, 224108.

[8] F. Neese, *Wiley Interdiscip. Rev.:Comput. Mol. Sci.*, 2022, **12**, e1606.

[9] K. Raghavachari, G. W. Trucks, J. A. Pople and M. Head-Gordon, *Chem. Phys. Lett.*, 1989, **157**, 479–483.

[10] H. F. Bettinger and O. Hauler, *Beilstein J. Org. Chem.*, 2013, **9**, 761–766.

[11] P. H. P. Harbach, M. Wormit and A. Dreuw, *J. Chem. Phys.*, 2014, **141**, 064113.

[12] J.-D. Chai and M. Head-Gordon, *Phys. Chem. Chem. Phys.*, 2008, **10**, 6615–6620.

[13] E. Epifanovsky, A. T. B. Gilbert, X. Feng, J. Lee, Y. Mao, N. Mardirossian, P. Pokhilko, A. F. White, M. P. Coons, A. L. Dempwolff, Z. Gan, D. Hait, P. R. Horn, L. D. Jacobson, I. Kaliman, J. Kussmann, A. W. Lange, K. U. Lao, D. S. Levine, J. Liu, S. C. McKenzie, A. F. Morrison, K. D. Nanda, F. Plasser, D. R. Rehn, M. L. Vidal, Z.-Q. You, Y. Zhu, B. Alam, B. J. Albrecht, A. Aldossary, E. Alguire, J. H. Andersen, V. Athavale, D. Barton, K. Begam, A. Behn, N. Bellonzi, Y. A. Bernard, E. J. Berquist, H. G. A. Burton, A. Carreras, K. Carter-Fenk, R. Chakraborty, A. D. Chien, K. D. Closser, V. Cofer-Shabica, S. Dasgupta, M. de Wergifosse, J. Deng, M. Diedenhofen, H. Do, S. Ehlert, P.-T. Fang, S. Fatehi, Q. Feng, T. Friedhoff, J. Gayvert, Q. Ge, G. Gidofalvi, M. Goldey, J. Gomes, C. E. González-Espinoza, S. Gulania, A. O. Gunina, M. W. D. Hanson-Heine, P. H. P. Harbach, A. Hauser, M. F. Herbst, M. Hernández Vera, M. Hodecker, Z. C. Holden, S. Houck, X. Huang, K. Hui, B. C. Huynh, M. Ivanov, A. Jász, H. Ji, H. Jiang, B. Kaduk, S. Kähler, K. Khistyaev, J. Kim, G. Kis, P. Klunzinger, Z. Koczor-Benda, J. H. Koh, D. Kosenkov, L. Koulias, T. Kowalczyk, C. M. Krauter, K. Kue, A. Kunitsa, T. Kus, I. Ladjánszki, A. Landau, K. V. Lawler, D. Lefrancois, S. Lehtola, R. R. Li, Y.-P. Li, J. Liang, M. Liebenthal, H.-H. Lin, Y.-S. Lin, F. Liu, K.-Y. Liu, M. Loipersberger, A. Luenser, A. Manjanath, P. Manohar, E. Mansoor, S. F. Manzer, S.-P. Mao, A. V. Marenich, T. Markovich, S. Mason, S. A. Maurer, P. F. McLaughlin, M. F. S. J. Menger, J.-M. Mewes, S. A. Mewes, P. Morgante, J. W. Mullinax, K. J. Oosterbaan, G. Paran, A. C. Paul, S. K. Paul, F. Pavošević, Z. Pei, S. Prager, E. I. Proynov, A. Rák, E. Ramos-Cordoba, B. Rana, A. E. Rask, A. Rettig, R. M. Richard, F. Rob, E. Rossomme, T. Scheele, M. Scheurer, M. Schneider, N. Sergueev, S. M. Sharada, W. Skomorowski, D. W. Small, C. J. Stein, Y.-C. Su, E. J. Sundstrom, Z. Tao, J. Thirman, G. J. Tornai, T. Tsuchimochi, N. M. Tubman, S. P. Veccham, O. Vydrov, J. Wenzel, J. Witte, A. Yamada, K. Yao, S. Yeganeh, S. R. Yost, A. Zech, I. Y. Zhang, X. Zhang, Y. Zhang, D. Zuev, A. Aspuru-Guzik, A. T. Bell, N. A. Besley, K. B. Bravaya, B. R. Brooks, D. Casanova, J.-D. Chai, S. Coriani, C. J. Cramer, G. Cserey, A. E. DePrince, III, R. A. DiStasio, Jr., A. Dreuw, B. D. Dunietz, T. R. Furlani, W. A. Goddard, III, S. Hammes-Schiffer, T. Head-Gordon, W. J. Hehre, C.-P. Hsu, T.-C. Jagau, Y. Jung, A. Klamt, J. Kong, D. S. Lambrecht, W. Liang, N. J. Mayhall, C. W. McCurdy, J. B. Neaton, C. Ochsenfeld,

J. A. Parkhill, R. Peverati, V. A. Rassolov, Y. Shao, L. V. Slipchenko, T. Stauch, R. P. Steele, J. E. Subotnik, A. J. W. Thom, A. Tkatchenko, D. G. Truhlar, T. Van Voorhis, T. A. Wesolowski, K. B. Whaley, H. L. Woodcock, III, P. M. Zimmerman, S. Faraji, P. M. W. Gill, M. Head-Gordon, J. M. Herbert and A. I. Krylov, *J. Chem. Phys.*, 2021, **155**, 084801.

[14] A. D. Becke, *J. Chem. Phys.*, 1993, **98**, 1372–1377.

[15] T. H. Dunning, Jr., *J. Chem. Phys.*, 1989, **90**, 1007–1023.